Psychoradiology, 2023, **3**, 1–11
DOI: 10.1093/psyrad/kkad008
Advance access publication date: 13 June 2023
Research Article

Structural and functional differences in the brains of patients with MCI with and without depressive symptoms and their relations with Alzheimer's disease: an MRI study

Rodolfo Dias Chiari-Correia[1,*], Vitor Tumas[1], Antônio Carlos Santos[2] and Carlos Ernesto G Salmon[3]

[1]Department of Neurosciences and Behavioral Sciences, Ribeirao Preto Medical School, University of Sao Paulo, 3900 Bandeirantes Avenue, Ribeirao Preto SP, 14040-900, Brazil
[2]Department of Medical Imaging, Hematology and Clinical Oncology, Ribeirao Preto Medical School, University of Sao Paulo, 3900 Bandeirantes Avenue, Ribeirao Preto SP, 14040-900, Brazil
[3]Department of Physics, Faculty of Philosophy, Sciences and Letters, University of Sao Paulo, 3900 Bandeirantes Avenue, Ribeirao Preto SP, 14040-900, Brazil
*Correspondence: Rodolfo Dias Chiari-Correia, rodolfodcorreia@alumni.usp.br

Abstract

Background: The mild cognitive impairment (MCI) stage among elderly individuals is very complex, and the level of diagnostic accuracy is far from ideal. Some studies have tried to improve the 'MCI due to Alzheimer's disease (AD)' classification by further stratifying these patients into subgroups. Depression-related symptoms may play an important role in helping to better define the MCI stage in elderly individuals.

Objective: In this work, we explored functional and structural differences in the brains of patients with nondepressed MCI (nDMCI) and patients with MCI with depressive symptoms (DMCI), and we examined how these groups relate to AD atrophy patterns and cognitive functioning.

Methods: Sixty-five participants underwent MRI exams and were divided into four groups: cognitively normal, nDMCI, DMCI, and AD. We compared the regional brain volumes, cortical thickness, and white matter microstructure measures using diffusion tensor imaging among groups. Additionally, we evaluated changes in functional connectivity using fMRI data.

Results: In comparison to the nDMCI group, the DMCI patients had more pronounced atrophy in the hippocampus and amygdala. Additionally, DMCI patients had asymmetric damage in the limbic-frontal white matter connection. Furthermore, two medial posterior regions, the isthmus of cingulate gyrus and especially the lingual gyrus, had high importance in the structural and functional differentiation between the two groups.

Conclusion: It is possible to differentiate nDMCI from DMCI patients using MRI techniques, which may contribute to a better characterization of subtypes of the MCI stage.

Keywords: mild cognitive impairment; depressive disorders; Alzheimer's Disease; neuroimaging

Introduction

Patients with mild cognitive impairment (MCI) have an evident cognitive decline that differentiates them from cognitively healthy individuals, but is mild enough to not be characterized as a specific form of dementia. In elderly individuals, MCI is also known as a transitional stage between healthy ageing and dementia such as Alzheimer's disease (AD) (Albert *et al.*, 2011).

One of the most commonly used set of diagnostic criteria to diagnose MCI are the recommendations from the National Institute on Ageing and Alzheimer's Association for MCI due to AD (Albert *et al.*, 2011). However, in routine clinical practice, it is a complex and comprehensive diagnosis. The variability of the symptoms due to their recent onset, their mild presentation, or the absence of biomarkers with less subjectivity causes an important impact on diagnostic accuracy. For example, in a recent study using amyloid positron emission tomography, which is one of the biomarkers for AD, only ∼55% of individuals diagnosed with MCI were considered positive for amyloid (Rabinovici *et al.*, 2019), which indicates that even MCI due to AD is a heterogeneous classification that needs to be further specified.

Some studies using neuropsychological tests and cluster techniques have progressed to better characterize the clinical stage of MCI, and it has been divided into more specific subtypes (Edmonds *et al.*, 2015; Machulda *et al.*, 2019). There are three commonly studied subtypes: amnestic MCI with only memory impairment; dysexecutive MCI with impairment in executive functions other than memory, attention and naming; and dysnomic MCI with a significant deficit in memory and naming. In another line of research, some studies have identified subtypes based on brain atrophy or tau protein accumulation in AD patients, which can also be identified in MCI due to AD (Whitwell *et al.*, 2012; Ferreira *et al.*, 2017). Three main subtypes were identified: typical AD with alterations in the medial temporal lobe and in regions of the associative cortex; limbic-predominant AD with higher alterations

Received: 17 February 2023; **Revised:** 19 May 2023; **Accepted:** 12 June 2023

in the hippocampus; and hippocampus-sparing AD with higher alterations in the associative cortex.

Another factor that contributes to MCI heterogeneity is codominance with other diseases that affect the brain, such as neurovascular and psychiatric diseases, with depressive disorder being one of the most frequent. Depression-related symptoms have a high prevalence in older adults diagnosed with MCI, between 20 and 50% (Zubenko *et al.*, 2003; Leyhe *et al.*, 2017), and cognitive decline is a typical comorbidity in older adults with major depression (Alexopoulos *et al.*, 2000). In addition, older adults with depression and MCI are more likely to convert to AD (Gabryelewicz *et al.*, 2007). However, late-life depression (LLD), i.e. major depression in elderly individuals, is normally considered an exclusion factor for the diagnosis of MCI due to AD because depression is also a primary cause of cognitive decline. Therefore, there are few studies on MCI that consider the influence of depressive symptoms on their analyses. However, individually, studies with magnetic resonance imaging (MRI) have consolidated advances to map the structural and functional alterations in the brains of individuals with AD and LLD.

Hippocampal atrophy is one of the most common MRI signs in patients with AD and MCI (Du *et al.*, 2001). Hippocampal atrophy is also a common MRI sign inpatients with LLD (Bell-McGinty *et al.*, 2002; Du *et al.*, 2014), but its intensity is lower than among patients with AD (Joko *et al.*, 2016). Atrophy in other medial temporal lobe regions, such as the amygdala, can also be found in AD, MCI, and LLD (Du *et al.*, 2014; Tabatabaei-Jafari *et al.*, 2015). Although posterior cingulate/precuneus atrophy that is typical in AD and in MCI (Jacobs *et al.*, 2012) does not appear to be as common in LLD (Ribeiz *et al.*, 2013), the reduction in the frontal areas and the increase in the lingual gyrus volumes in LLD (Ribeiz *et al.*, 2013; Du *et al.*, 2014) are not as commonly seen in MCI or in the early typical AD stage.

In diffusion tensor imaging (DTI) studies, which can be used to analyse the microstructure of the white matter and its organization, uncinate fasciculus and cingulate tract degeneration was associated with medial temporal lobe atrophy both in MCI (Liu *et al.*, 2011; Sun *et al.*, 2014) and LLD (Wen *et al.*, 2014). Otherwise, lower white matter integrity in the fornix and posterior corpus callosum (splenium) fibres appear to be related to MCI (Liu *et al.*, 2011; Sun *et al.*, 2014), as in the anterior corpus callosum (genu) and anterior cingulum to LLD (Bae *et al.*, 2006).

In studies using MRI functional connectivity (FC), which measures aspects such as the intensity that spatially apart brain regions functionally connect to each other to perform a task, there is a common pattern of changes in AD participants' brains. Mainly, the default mode network decreases its intrinsic and extrinsic connectivity, while the salience network acts inversely, increasing its connectivity (Brier *et al.*, 2012; Balthazar *et al.*, 2014). A similar pattern is observed in MCI due to AD participants (Badhwar *et al.*, 2017). In LLD patients, alterations in FC are not consistent; however, high FC within the default mode network (Alexopoulos *et al.*, 2012) and low FC within the salience (Yuen *et al.*, 2014) and executive control (Alexopoulos *et al.*, 2012) networks, as well as local changes in the dorsolateral prefrontal cortex (Alexopoulos *et al.*, 2012), and in the anterior cingulate (Yuen *et al.*, 2014), are some of the most common findings in the literature.

As mentioned earlier, the stage known as MCI is very heterogeneous within the elderly population and may have different causes, symptoms, and treatments. Some studies have tried to improve this classification by stratifying these patients into subgroups, and we believe that depression symptoms among elderly patients may play an important role in helping to better define the MCI group. Additionally, although MCI, AD, and LLD patients have been more extensively studied using MRI, few studies have sought to define these changes in patients with MCI who do not meet the criteria for major depression but still have moderate and persistent depressive symptoms. Therefore, the following questions arise. Based exclusively on the neuroimaging findings, is it possible to differentiate the brains of nondepressed MCI (nDMCI) from those who have depression symptoms and MCI (DMCI)? If possible, which is our current hypothesis, and considering that patients with concomitant MCI and depressive symptoms are at higher risk of converting to AD, do these differences between nDMCI and DMCI have similarities to brain changes already known in AD?

In this context, we used MRI multimodality techniques that have been shown to enhance the ability to characterize brain structures and analyse brain functionality (Lin *et al.*, 2012; Hao *et al.*, 2013; Salvador *et al.*, 2019) to analyse structural and functional brain changes in MCI patients with and without depressive symptoms. We also compared these two groups with cognitively normal older adults (CN) and AD patients.

Methods

Participants

Sixty-five participants divided into four groups were enrolled in this retrospective cross-sectional study at the University Clinical Hospital. The investigation was approved by the hospital ethics committee, and all participants provided informed consent. Clinical evaluations and MR exams were performed between 2014 and 2017, and patients with MCI and AD were diagnosed following the criteria by the National Institute on Ageing and Alzheimer's Association (Albert *et al.*, 2011; McKhann *et al.*, 2011). Depression severity was evaluated using the Geriatric Depression Scale Short Form-15 (GDS) (Yesavage and Sheikh, 1986), and cognitive impairment status was evaluated by the Clinical Dementia Rating (CDR) (Hughes *et al.*, 1982) and Mini-Mental State Examination (MMSE) (Folstein *et al.*, 1975).

For all groups, the exclusion criteria were as follows: <4 years of education, age below 60 or above 90 years, Hachinski scale over 3, presence of other systemic disorders associated with cognitive decline, and potentially clinically significant abnormalities (e.g. silent strokes, aneurysms, and tumoral formations) accidentally detected on MRI. CN participants could not have any clinical cognitive or psychiatric disorders and had CDR = 0 and GDS ≤ 4. Patients with MCI were divided into two groups, i.e. depressed and nondepressed, based on the following criteria: the members of the nDMCI group were participants without a history of depression. In addition, they could not have a score >4 on the GDS in the period of at least 1 year before the MRI exam. Participants in the DMCI group had recent mild to moderate depressive symptoms. These participants had a score ≥5 and ≤10 on the GDS. Of the 14 individuals in the DMCI group, five were receiving antidepressant monotherapy (selective serotonin reuptake inhibitors), and two were receiving combination treatment between selective serotonin reuptake inhibitors and benzodiazepines. Individuals who met the DSM-V criteria (Marty and Segal, 2015) for major depression (MD) were excluded due to the MCI diagnostic criteria we used (Albert *et al.*, 2011) and because depression could be the primary cause of MCI among those individuals.

MRI acquisition

All images were acquired using a 3T MR scanner (Achieva, Philips Medical) and a head coil with eight channels. High-resolution

Table 1: Main demographic and clinical data (mean ± standard deviation) divided by groups.

	CN ($n = 19$)	nDMCI ($n = 17$)	DMCI ($n = 15$)	AD ($n = 14$)
Age (years)	70.5 (6.9)	74.2 (6.8)	73.7 (6.6)	75.2 (8.6)
Education (years)	9.9 (5.0)	7.7 (5.4)	8.9 (6.2)	6.1 (2.7)
MMSE	27.7 (1.9)	25.6 (2.5)	26.0 (3.7)	20.8 (2.7)*
GDS	2.4 (2.3)	2.2 (1.5)	7.5 (1.6)*	2.6 (1.6)
CDR	0	0.5	0.5	1
Sex	13F	12F	10F	10F

*A significant difference between groups ($P < 0.001$) based on ANOVA with Fisher's LSD method.

anatomical images (3DT1) were captured using an MPRAGE sequence (TR/TE = 2500/3.2 ms, 7.0 ms time echo spacing, 900 ms inversion time, voxel size = 1 × 1 × 1 mm^3, flip angle = 8°, FOV = 240 × 240 mm^2, and 160 slices). Resting-state functional magnetic resonance images (eyes open, no fixation) from each participant were acquired using an EPI sequence with the following parameters: 2000 ms repetition time, 30 ms echo time, 240 × 240 mm field of view, 3 × 3 mm in-plane voxel size, 4.0 mm slice thickness, 0.5 mm slice gap, 32 slices, 80° flip angle, 200 volumes, 25.2 Hz bandwidth per pixel. DTI were also acquired using a spin–echo-EPI sequence with the following parameters: TR/TE = 9300/54 ms, pixel size = 2 × 2 mm^2, slice thickness = 2 mm, EPI factor = 67, FOV = 256 × 256 mm^2, acquisition matrix = 128 × 128 pixels, 60 slices, 33 volumes, 32 with diffusion gradients ($b = 1000$ s/mm^2) and one with $b = 0$, and overplus = no.

Morphometric assessment

Regional cortical thickness and brain regional volumes were obtained by FreeSurfer software (Fischl *et al.*, 2002) (v.6.0) using the Desikan–Killiany Atlas. We chose the regions of interest (ROI) on the basis of previous MRI studies on AD, MCI, and LLD. The ROI chosen were frequently associated with the psychopathology of these diseases, as seen in the studies cited in the Introduction section (Bell-McGinty *et al.*, 2002; Jacobs *et al.*, 2012; Ribeiz *et al.*, 2013; Du *et al.*, 2014; Tabatabaei-Jafari *et al.*, 2015; Joko *et al.*, 2016). The ROI analysed are listed in the Supplementary Material.

White matter assessment

Diffusion-weighted data were processed using the FMRIB Software Library (https://fsl.fmrib.ox.ac.uk/fsl/) pipeline. The data were corrected for eddy current distortion/head motion, and the brain was extracted using eddy current corrections and brain extraction tools. Fractional anisotropy, mean diffusivity (MD), axial diffusivity (AxD), and radial diffusivity (RD) were calculated and arranged in brain maps by DTIFit software.

For the white matter analysis, we used the TRACULA (TRActs Constrained by UnderLying Anatomy) tool (Yendiki *et al.*, 2011). It is part of FreeSurfer's package and uses global probabilistic tractography from FSL combined with an Atlas and other FreeSurfer segmentations and parcellations to obtain eighteen tracts. The name of the tracts can be seen in the Supplementary Material.

FC

Functional MRI data were processed using the CONN FC toolbox (Whitfield-Gabrieli and Nieto-Castanon, 2012). The complete default pipeline, including motion correction and outlier identification, was performed, as well as spatial smoothing with a Gaussian filter of 6 mm. We performed an ROI-to-ROI analysis and chose to use the AAL atlas (Tzourio-Mazoyer *et al.*, 2002) to define the ROI. The AAL atlas is commonly used in FC studies, which would make it easier to compare our results to the existing literature in this field. For each ROI defined, an averaged functional time series was calculated, and then a Pearson correlation coefficient was estimated for each pair of ROI.

Statistical analysis

The regional volumes were normalized by dividing by the total intracranial volume to reduce the effects of variations related to the size of the head of each participant. One-way ANOVA with Fisher's LSD method was used to find the difference between groups in relation to demographic data such as age, MMSE, GDS, and years of education. The same statistical test was used in the comparison between groups in volume and cortical thickness, as well as in the diffusibility metrics (FA, MD, AxD, and RD). In all these cases, we used $P < 0.05$. For cases where the data distribution within a group did not follow the normality criteria, the nonparametric Kruskal–Wallis test with the pairwise method of multiple comparisons was used. In functional connectivity analysis, we used t-statistics with a threshold of $P < 0.05$ corrected with the false discovery rate method in group analysis.

We used Pearson's linear correlation coefficient with $P < 0.05$ to analyse the GDS and MMSE correlation to the neuroimaging findings. Last, we used the following equation to calculate the asymmetry index in the uncinate fasciculus: [(left − right)/(left + right)] × 200.

Results

Sample demographics

From the 82 individuals selected initially, six were excluded because they had a low level of education (<4 years), two were excluded because they had major depression, three were excluded because they had been diagnosed with non-initial AD (CDR2), and six were excluded because they had been diagnosed with other types of dementia (mixed or frontotemporal dementia). The final study sample was composed of 65 participants divided into four groups: 19 in the CN group, 17 in the nDMCI group, 15 in the DMCI group, and 14 in the AD group. The demographic information of all participants divided by groups is presented in Table 1. There were no significant differences among groups in age and years of education. As expected, the AD group had a lower mean value on the MMSE ($F = 18.59$, $P < 0.0001$), and GDS scores were significantly higher ($F = 27.33$, $P < 0.0001$) in the DMCI participants. Although the groups are not symmetrical in relation to the number of males and females, they were paired because the number of females was between 2 and 2.5 times the number of males in all groups.

Figure 1: Normalized brain volumes (mean ± standard deviation) of the right/left hippocampus, amygdala, lingual gyrus, and the isthmus of the cingulate gyrus are expressed as a percentage of the intracranial volume for the CN, nDMCI, DMCI, and AD groups. Significant differences ($P < 0.05$) are marked as follows: a when different from the CN group; b when different from the nDMCI group; c when different from the DMCI group; and d when different from the AD group.

Morphometric analysis

Volume

In the hippocampus and amygdala, the average volume of each group followed the pattern CN > nDMCI > DMCI > AD (Fig. 1). However, considering the statistical test ($P < 0.05$), the DMCI and AD groups had a lower volume in the hippocampus in both regions and hemispheres than the CN group. The AD group also had lower volumes in the bilateral hippocampus and amygdala than the nDMCI group (Fig. 1).

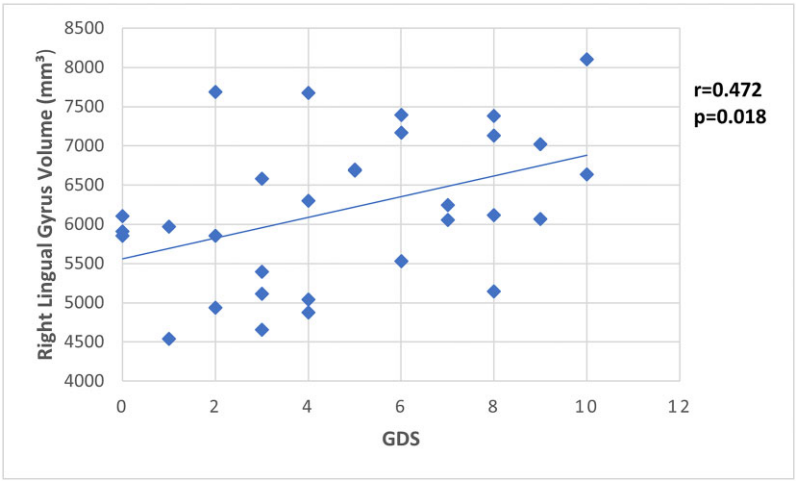

Figure 2: Correlation between the right lingual gyrus volume and scores on the GDS. The blue line represents the linear regression between the data, with the Pearson correlation coefficient and the *P* value of this association being indicated in the upper right.

On the other hand, in the lingual gyrus and in the isthmus of the cingulate gyrus, the average volumes followed the pattern CN ≅ DMCI > nDMCI > AD. The statistical test in these two regions showed that the AD and nDMCI groups had lower volumes in the left isthmus of the cingulate gyrus and in the right lingual gyrus than the DMCI and CN groups (Fig. 1). In the left lingual gyrus, the nDMCI and AD groups had a lower volume than the CN group.

The corpus callosum volume was higher in the CN group than in all other groups in the middle posterior and anterior portions. It was also higher in the central and middle anterior portions compared to the DMCI and AD groups and higher than only the AD group in the posterior portion of the CC.

Total brain volume without ventricles had no significant differences between groups. However, the DMCI group volume average was closer to CN than the nDMCI group. The averages in 10^4 cm^3 were CN = 97.7 (12.1), nDMCI = 92.1 (7.0), DMCI = 95.4 (8.4), and AD = 89.9 (8.4).

White matter hypointensity volume was higher in the AD group than in the CN group but was not different between the nDMCI and DMCI groups.

As we found a statistical difference between the DMCI and nDMCI groups in the volume of the left isthmus of the cingulate and right lingual gyrus, we calculated a correlation between these measurements and the GDS and MMSE scales. In patients with MCI (nDMCI and DMCI), the GDS score was positively correlated ($r = 0.472$ and $P = 0.018$) with the lingual gyrus volume (Fig. 2). No correlation was found between the left isthmus of the cingulate and the GDS. When we considered all 65 research participants, the correlation between the GDS and the lingual gyrus volume was not statistically significant. There was also no correlation observed of the volume of the right lingual gyrus and the left isthmus of the cingulate with the MMSE score.

Cortical thickness

The DMCI group had an average cortical thickness closer to that of the CN group in the left entorhinal cortex than in the right hemisphere (Fig. 3). In the lingual gyrus, the result in cortical thickness was similar to the volume analysis in this region with the pattern CN ≅ DMCI > nDMCI > AD. The nDMCI group as well as the AD group had lower cortical thickness than the CN group in both hemispheres (Fig. 3).

The cortical regions of the precuneus, isthmus of the cingulate gyrus, and parahippocampal gyrus had bilaterally higher cortical thickness in the CN group than in the AD group.

DTI analyses

Tractography of major tracts

The MD and RD in the left UNC of the nDMCI group were higher than those of the CN group in the statistical test (Fig. 4). On the other hand, the MD was higher in the DMCI group in the right hemisphere than in the CN group (Fig. 4). The MD and RD values in all groups had higher average values in the right hemisphere compared to the left hemisphere in the UNC (Fig. 4). However, the degree of asymmetry was highest in the DMCI group and lowest in the nDMCI group. This is evident when we look at the asymmetry indexes whose values for CN, nDMCI, DMCI, and AD were, respectively: −1.59, −0.47, −2.36, and −2.07 for MD and −2.22, −0.60, −3.77, and −3.08 for RD.

In the comparison between the CN and AD groups, the FA, MD, and RD were bilaterally different in the UNC. The MD and RD in the right ILF and the AxD in the right SLFT and SLFP were higher in the AD group. Finally, RD in the right CAB was higher in the AD group as well.

FC

The FC between the analysed ROI in the CN group had no statistically significant changes in comparison with the nDMCI and DMCI groups. However, 20 connections had higher FC values in the CN group than in the AD group (Fig. 5). As the FC analysis was performed in pairs, we also compared the DMCI and nDMCI groups in relation to the AD group. Three connections had concomitantly higher FC in the CN, DMCI, and nDMCI groups than in the AD group (L_HIP—R_PHG; R_HIP—L_THA; L_REC—L_TPO). Additionally, compared to the AD group, the CN shared with the nDMCI group a higher FC in the R_ANG—L_REC connection and with the DMCI group in the L_MFG—L_SMG connection. Finally, compared to the AD group, the FCs that were higher exclusively in patients with MCI were (L_REC—R_PHG; R_REC—R_ANG) in the nDMCI group and (R_LING—R_PHG; R_LING—L_PHG; L_ LING—L_PHG) in the DMCI group (Fig. 5).

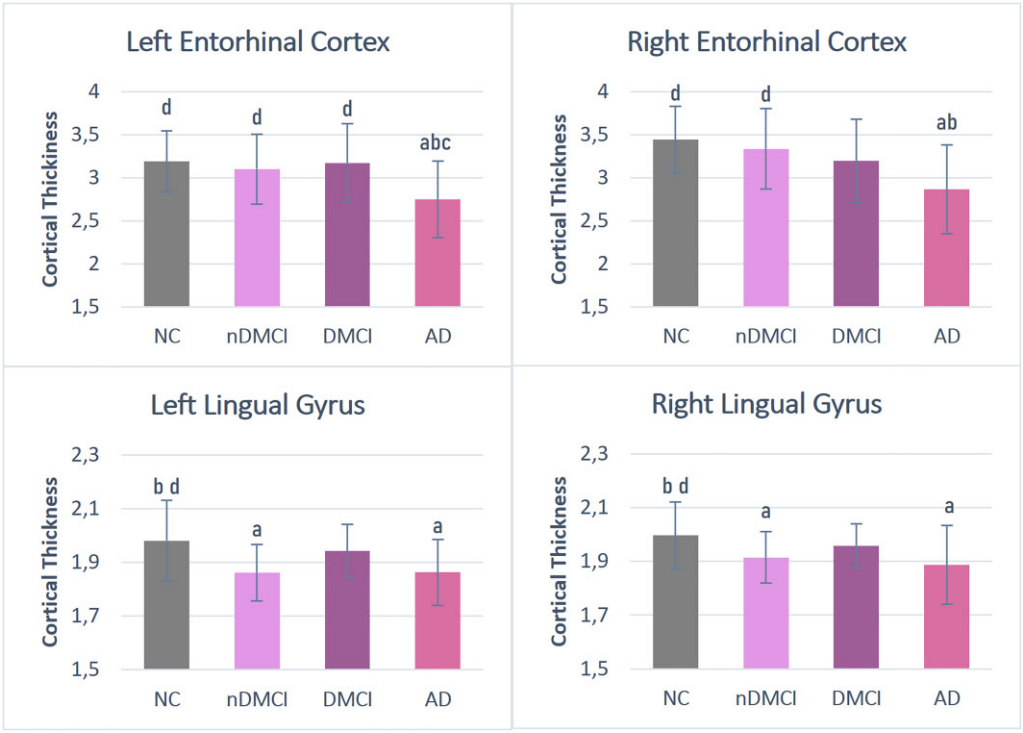

Figure 3: Cortical thickness values (mean ± standard deviation) of the entorhinal cortex and lingual gyrus for the CN, nDMCI, DMCI, and AD groups. Significant differences ($P < 0.05$) are marked as follows: a when different from the CN group; b when different from the nDMCI group; c when different from the DMCI group; and d when different from the AD group.

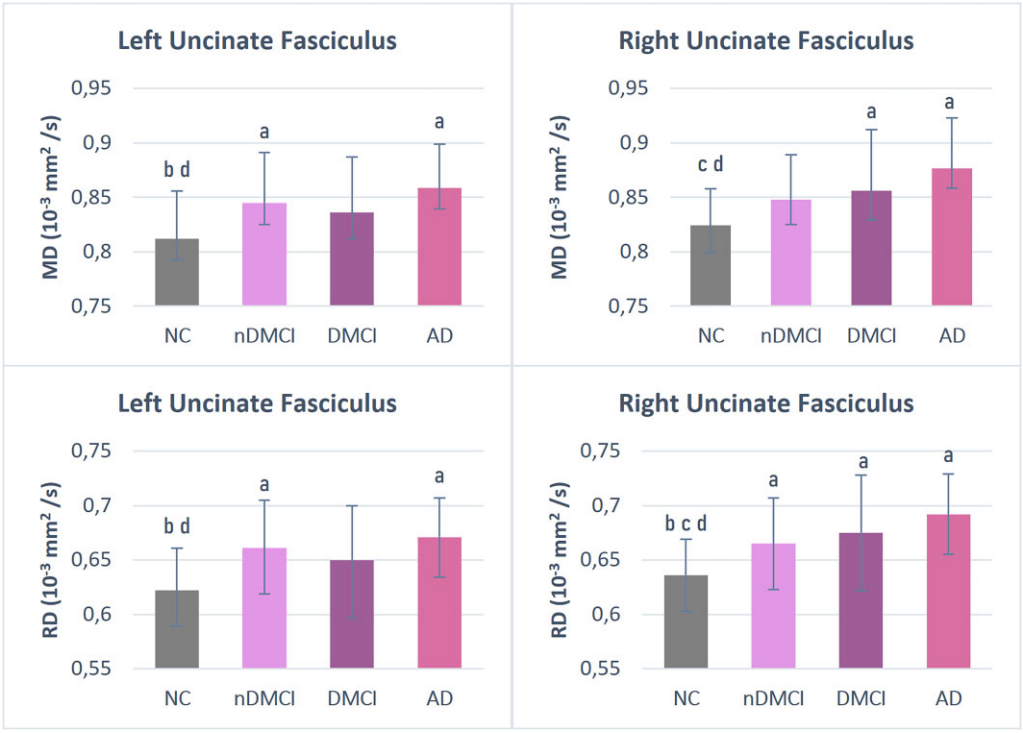

Figure 4: Fractional anisotropy (FA) and RD (mean ± standard deviation) of the uncinate fasciculus for the CN, nDMCI, DMCI, and AD groups. Significant differences ($P < 0.05$) are marked as follows: a when different from the CN group; b when different from the nDMCI group; c when different from the DMCI group; and d when different from the AD group.

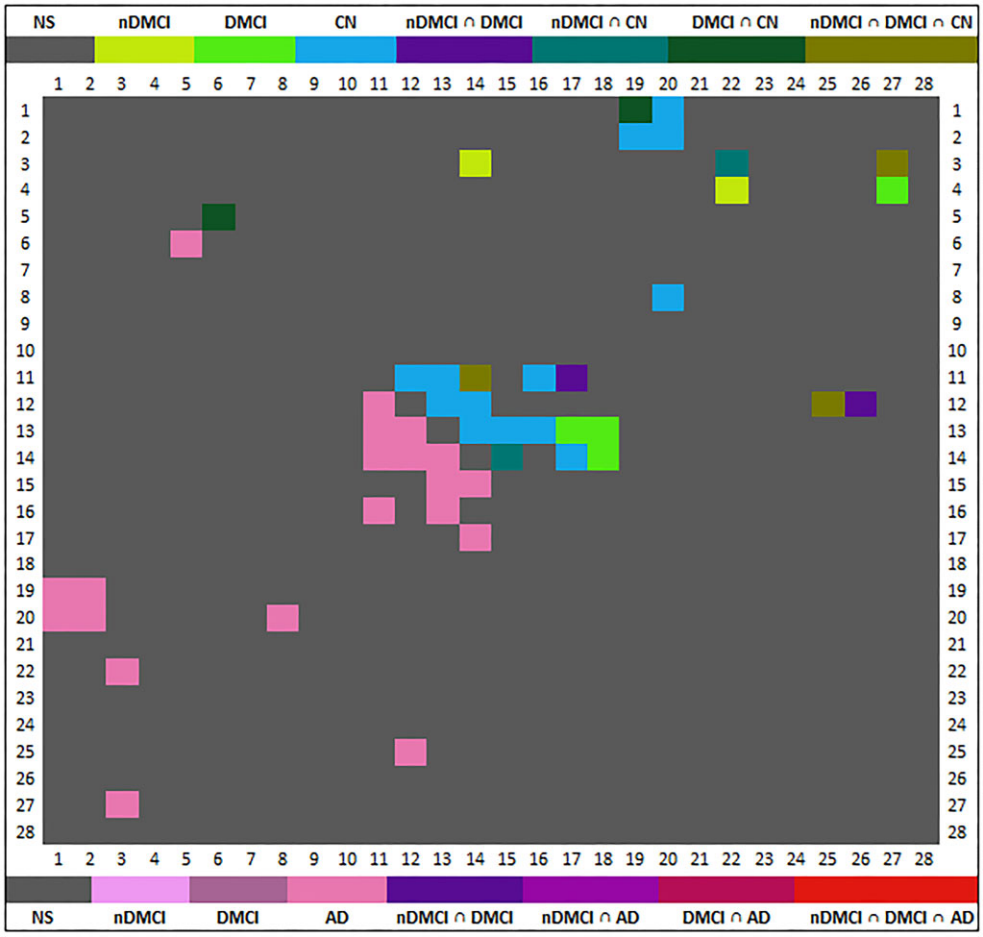

Figure 5: Elements represent connections that were significantly different (*P* false discovery rate < 0.05) in the group comparison. The lower diagonal shows connections with higher FC in the CN compared to the nDMCI, DMCI, and AD groups. The upper diagonal shows connections with higher FC in the CN, nDMCI, and DMCI groups than in the AD group. Regions: 1–2 middle frontal gyrus L/R (MFG), 3–4 rectus L/R (REC), 5–6 insula L/R (INS), 7–8 anterior cingulate L/R (ACG), 9–10 posterior cingulate L/R (PCG), 11–12 hippocampus L/R (HIP), 13–14 parahippocampal gyrus L/R (PHG), 15–16 amygdala L/R (AMYG), 17–18 lingual gyrus L/R (LING), 19–20 supramarginal L/R (SMG), 21–22 angular L/R (ANG), 23–24 precuneus L/R (PCUN), 25–26 thalamus L/R (THA), and 27–28 temporal pole L/R (TPO). NS = no statistical significance.

Discussion

The medial temporal lobe is a key region for both AD (Braak and Braak, 1991; Ramos Bernardes da Silva Filho *et al.*, 2017) and LLD (Du *et al.*, 2014; Linnemann and Lang, 2020) and is one of the first and most strongly affected regions during AD progression. In our results, the DMCI group had lower volumes in the hippocampus and amygdala than the control group but still had lower intensities than the initial AD patients. This more accentuated decrease in hippocampal volume in depressed elderly individuals follows the findings of other studies, both in the case of elderly individuals with (Chung *et al.*, 2016) and without cognitive impairment (Bell-McGinty *et al.*, 2002). Therefore, our findings and those of previous studies suggest that the pathophysiological mechanisms related to depressive symptoms in elderly individuals could be directly associated with the causes of this extra atrophy in the hippocampus. However, further confirmation is needed through longitudinal studies with a larger sample size.

The main structural differences between the nDMCI and DMCI groups were in the medial posterior areas of the brain (Fig. 1), with significant differences in the lingual gyrus and the isthmus of the cingulate gyrus. The average values of cortical thickness and volume in these areas were very close to controls in the DMCI group, unlike what we observed in the nDMCI group. Additionally, the lingual gyrus had a positive correlation with the values of the Geriatric Depression Scale (Fig. 2). The combination of higher hippocampal atrophy and lingual gyrus structural preservation seems to be a key factor in depressive symptoms in elderly people with MCI. Our findings suggest that the lingual gyrus may be an area of the brain that also has marked atrophy in the early stages of typical AD, as well as neighbouring regions in the temporal lobe; however, this finding is not commonly found in the reviewed literature. We believe that this difference can be explained because in most of the studies, there was no special attention given to depressed individuals in the MCI and AD groups or consideration of the possibility of different types of atrophy in AD. Thus, these individuals had the lingual gyrus volume preserved and thus increased the mean of the group and decreased the chance of the volumetric reduction being detected. The lingual gyrus is a region of the occipital lobe generally associated with visual memory and facial and spatial recognition (Kozlovskiy *et al.*, 2014), which are functions that are known to be impaired with the advancement of Alzheimer's disease. Atrophy of the lingual gyrus has also been linked to poor performance in neurocognitive testing and the response to antidepressants in patients with major depression (Jung *et al.*, 2014).

The volume of the middle and mid-anterior sections of the corpus callosum was lower in the DMCI group compared to the CN group. This difference was not observed in the nDMCI group. The literature has divergent results on CC volumetric analysis in patients with depression. The size and volume of the corpus callosum can vary compared to normal controls, with some studies showing it to be smaller (Hahn *et al.*, 2015; Ran *et al.*, 2020), preserved (Emsell *et al.*, 2017), or even larger (Wu *et al.*, 1993). In studies indicating volumetric loss, it is frequently observed in the anterior region, which is consistent with our findings. The anterior corpus callosum connects prefrontal cortex hemispheres, and abnormalities in this region can impact working memory, mood, and emotional processing. (Bae *et al.*, 2006).

On examining the microstructure of white matter using tractography, we observed the most significant results in distinguishing between the nDMCI and DMCI groups on the UNC. The UNC connects parts of the limbic system to the orbitofrontal cortex. This finding may be aligned with our morphometric analyses in which limbic regions had a decrease in cortical volume in the DMCI group compared to the CN group. Also, we noticed an asymmetry on the white matter microstructure with the DTI scalars pointing to more integrity on the left hemisphere in all groups. However, the asymmetry was more pronounced in the DMCI group and less noticeable in the nDMCI group. The higher white matter microstructure integrity on the left side concurs with previous findings in the literature (Honnedevasthana Arun *et al.*, 2021). Nonetheless, it is far from consensus and seems not to have a relation to handedness (Honnedevasthana Arun *et al.*, 2021; López-Vicente *et al.*, 2021). Previous studies indicates a correlation between reduced integrity of white matter microstructure in the UNC and LLD (Colloby *et al.*, 2011; Wen *et al.*, 2014). Nevertheless, we only found one study investigating the relationship between higher asymmetry in UNC and depressive symptoms, pointing to a non-association (Zhang *et al.*, 2012).

Based on the ILF anatomy and its lingual branch, connecting the lingual gyrus and anterior temporal lobe (Herbet, Zemmoura and Duffau, 2018), we had higher expectations for more expressive results, due to lingual gyrus results on the morphometric analysis. Although no statistical differences were found in the ILF, we observed a trend that was consistent with the morphometric analysis in the DMCI group, with virtually all DTI metrics (FA, MD, AxD, and RD) being closer to those of the control group than in the nDMCI group, as can be seen in the Supplementary material. The impact of the lingual branch may have been weakened in the average ILF value due to the presence of other ILF branches. This could potentially be why the difference between groups in the ILF was not detectable by the statistical test.

In the functional analysis, the changes in connectivity between the AD and CN groups were mainly between regions of the medial temporal lobe, such as the hippocampus, amygdala, and parahippocampal gyrus. There were no significant differences in FC between the nDMCI and DMCI groups, nor when comparing both groups to the normal control group. Otherwise, compared to the AD group, the hippocampus and parahippocampus had FC increased with the lingual gyrus in the DMCI group. The lingual gyrus naturally has a high positive FC with the hippocampus (Hao *et al.*, 2020), but in the DMCI group, we observed hyperconnectivity of these connections since the CN group did not have a higher FC in the same places compared to the AD group (Fig. 5). The lingual gyrus was structurally preserved and highly connected to the hippocampus in the DMCI group. Thus, we can hypothesize the lingual gyrus may be used in a compensatory neuronal process to minimize the functional loss due to the higher hippocampal atrophy.

Based on our findings, the DMCI group was characterized by higher atrophy than the nDMCI group in the hippocampus and amygdala, with the volume of these regions being significantly different from that of the CN group, structural preservation of the isthmus of the cingulate and lingual gyrus, and higher asymmetry between hemispheres in the uncinate fasciculus. These characteristics suggest that in the context of brain atrophy, our DMCI group could not be related to the typical AD pattern, which commonly has atrophy in the posterior medial regions, with our AD group included, but it may still be related to the limbic-predominant subtype.

Limbic-predominant AD has a later onset, a slower disease progression, and a predominance among females (Ferreira *et al.*, 2020). It is also associated with LLD (Cheung and Mui, 2021). However, previous studies (Byun *et al.*, 2015; Ferreira *et al.*, 2017) on these AD subtypes found no association between depressive symptoms and a subtype. We believe this was because the databases used in these studies excluded not only patients with a diagnosis of major depression but also patients indicating any degree of depression. A commonly used inclusion criterion is GDS ≤ 5.

To the best of our knowledge, this is the first study that has carried out a direct comparison in terms of structural and functional analysis based on images between participants with non-depressed MCI and MCI with depressive symptoms. Our findings contribute to a better understanding of the brain changes related to MCI conditions and the progression to dementia; however, some limitations can be identified in our study. More participants in each group and a longitudinal study model could improve our ability to answer our main questions. Evident vascular dysfunction was used as an exclusion criterion; however, vascular pathologies have been closely related to both AD and LLD (Herrmann *et al.*, 2008), and the absence of these patients can hide important effects in differentiating between pathologies. However, we compared the number of white matter lesions in each group. These lesions originated most often from small vessel diseases and other vascular dysfunctions, and we found no differences between the nDMCI and DMCI groups.

In our study, we observed that patients with nDMCI and DMCI may present different patterns of atrophy and functional alterations that can be differentiated by neuroimaging, with some medial posterior regions of the brain, with emphasis on the lingual gyrus, seeming to have a central role in differentiating these patients. The pattern we found in the DMCI group may not be associated with the typical AD pattern of atrophy but can still be linked to the predominant-limbic subtype with higher atrophy in limbic regions and higher associative cortex preservation, which would need further investigation. Owing to its limitations, we can consider that this study has a more exploratory design, pointing out new and important points of attention to help future studies better characterize the MCI subtypes.

Supplementary Data

Supplementary data are available at *Psychoradiology Journal* online.

Author Contributions

R.D.C.C.: conception and design, statistical analysis, drafting the manuscript and tables, and analysis and/or interpretation of data. C.E.G.S.: conception and design, revision of image acquisition and

processing protocol, and analysis and/or interpretation of data. A.C.S.: revision of image acquisition and processing protocol, critical revision of the article, and analysis and/or interpretation of data. V.T.: acquisition and analysis of clinical and neurophysiological data, and critical revision of the article. All authors discussed the results and contributed to the final manuscript.

Conflict of Interest

The authors declare no conflict of interests.

Funding

This study was partially funded by the University of Sao Paulo (NAPNA-USP) and partially by the Sao Paulo Research Foundation (FAPESP).

Acknowledgments

We thank the Brazilian research agencies FAPESP, CAPES, and CNPq for all their support during this work.

Data Availability

The data present in this submission has not been published and is not under consideration elsewhere. The data is not public and can be available upon reasonable request.

References

Albert MS, Dekosky ST, Dickson D, *et al.* (2011) The diagnosis of mild cognitive impairment due to Alzheimer's disease: recommendations from the National Institute on Aging-Alzheimer's Association workgroups on diagnostic guidelines for Alzheimer's disease. *Alzheimer's & Dement* **7**:270–9. doi:10.1016/j.jalz.2011.03.008

Alexopoulos GS, Meyers BS, Young RC, *et al.* (2000) Executive dysfunction and long-term outcomes of geriatric depression. *Arch Gen Psychiatry* **57**:285–90. doi:10.1001/archpsyc.57.3.285

Alexopoulos GS, Hoptman MJ, Kanellopoulos D, *et al.* (2012) Functional connectivity in the cognitive control network and the default mode network in late-life depression. *J Affect Disord* **139**:56–65. doi:10.1016/j.jad.2011.12.002

Badhwar A, Tam A, Dansereau C, *et al.* (2017) Resting-state network dysfunction in Alzheimer's disease: a systematic review and meta-analysis. *Alzheimer's Dement* **8**:73–85. doi:10.1016/j.dadm.2017.03.007

Bae JN, Macfall JR, Krishnan KRR, *et al.* (2006) Dorsolateral prefrontal cortex and anterior cingulate cortex white matter alterations in late-life depression. *Biol Psychiatry* **60**:1356–63. doi:10.1016/j.biopsych.2006.03.052

Balthazar MLF, Pereira FRS, Lopes TM, *et al.* (2014) Neuropsychiatric symptoms in Alzheimer's disease are related to functional connectivity alterations in the salience network. *Hum Brain Mapp* **35**:1237–46. doi:10.1002/hbm.22248

Bell-McGinty S, Butters MA, Meltzer CC, *et al.* (2002) Brain morphometric abnormalities in geriatric depression: long-term neurobiological effects of illness duration. *Am J Psychiatry* **159**:1424–27. doi: 10.1176/appi.ajp.159.8.1424

Braak H, Braak E (1991) Neuropathological stageing of Alzheimer-related changes. *Acta Neuropathol* **82**:239–59. doi:10.1007/BF00308809

Brier M, Thomas JB, Snyder AZ, *et al.* (2012) Loss of intra- and inter-network resting State functional connections with Alzheimer's Disease progression. *J Neurosci* **32**:8890–9. doi: 10.1523/JNEUROSCI.5698-11.2012

Byun MS, Kim SE, Park J, *et al.* (2015) Heterogeneity of regional brain atrophy patterns associated with distinct progression rates in Alzheimer's disease. *PLoS ONE* **10**:e0142756. doi:https://doi.org/10.1371/journal.pone.0142756

Cheung ESL, Mui AC (2021) Gender variation and late-life depression: findings from a national survey in the USA. *Ageing Int* **48**:263–80. doi:

Chung JK, Plitman E, Nakajima S, *et al.* (2016) Depressive symptoms and small hippocampal volume accelerate the progression to dementia from mild cognitive impairment. *J Alzheimer's Dis* **49**:743–54. doi:10.3233/JAD-150679

Colloby SJ, Firbank MJ, Thomas AJ, *et al.* (2011) White matter changes in late-life depression: a diffusion tensor imaging study. *J Affect Disord* **135**:216–20. doi:10.1016/j.jad.2011.07.025

Du AT, Schuff N, Amend D, *et al.*, (2001) Magnetic resonance imaging of the entorhinal cortex and hippocampus in mild cognitive impairment and Alzheimer's disease. *J Neurol Neurosurg Psychiatry* **71**:441–7. doi:10.1136/jnnp.71.4.441

Du M, Liu J, Chen Z, *et al.* (2014) Brain grey matter volume alterations in late-life depression. *J Psychiatry Neurosci* **39**:397–406. doi:10.1503/jpn.130275

Edmonds EC, Delano-Wood L, Clark LR, *et al.* (2015) Susceptibility of the conventional criteria for mild cognitive impairment to false-positive diagnostic errors. *Alzheimer's Dement* **11**:415–24. doi:10.1016/j.jalz.2014.03.005

Emsell L, Adamson C, De Winter F-L, *et al.* (2017) Corpus callosum macro and microstructure in late-life depression. *J Affect Disord* **222**:63–70. doi:10.1016/j.jad.2017.06.063

Ferreira D, Nordberg A, Westman E, *et al.* (2017) Distinct subtypes of Alzheimer's disease based on patterns of brain atrophy: longitudinal trajectories and clinical applications. *Sci Rep***7**:46263. doi:10.1038/srep46263

Ferreira D, Nordberg A, Westman E (2020) Biological subtypes of Alzheimer disease. *Neurology* **94**:436–48. doi:10.1212/WNL.0000000000009058

Fischl B, Salat DH, Busa E, *et al.* (2002) Whole brain segmentation: automated labeling of neuroanatomical structures in the human brain. *Neuron* **33**:341–55. doi: 10.1016/S0896-6273(02)00569-X

Folstein MF, Folstein SE, McHugh PR (1975) "Mini-Mental state". A practical method for grading the cognitive state of patients for the clinician. *J Psychiatr Res* **12**:189–98. doi:10.1016/0022-3956(75)90026-6

Gabryelewicz T, Styczynska M, Luczywek E, *et al.* (2007) The rate of conversion of mild cognitive impairment to dementia: predictive role of depression. *Int J Geriatr Psychiatry* **22**:563–7. doi:10.1002/gps.1716

Hahn C, Lim H–K, Won WY, *et al.* (2015) Sub-regional volumes changes of the corpus callosum in the drug naive patients with late-onset depression. *Prog Neuropsychopharmacol Biol Psychiatry* **56**:46–51. doi:10.1016/j.pnpbp.2014.07.008

Hao X, Xu D, Bansal R, *et al.* (2013) Multimodal magnetic resonance imaging: the coordinated use of multiple, mutually informative

probes to understand brain structure and function. *Hum Brain Mapp* **34**:253–71. doi:10.1002/hbm.21440

Hao ZY, Zhong Y, Ma ZJ, *et al.* (2020) Abnormal resting-state functional connectivity of hippocampal subfields in patients with major depressive disorder. *BMC Psychiatry* **20**:71. doi:10.1186/s12888-020-02490-7

Herbet G, Zemmoura I Duffau H (2018) Functional anatomy of the inferior longitudinal fasciculus: from historical reports to current hypotheses. *Front Neuroanatomy* **12**:77. doi:10.3389/fnana.2018.00077

Herrmann LL, Le Masurier M, Ebmeier KP (2008) White matter hyperintensities in late life depression: a systematic review. *J Neurol Neurosurg Psychiatry* **79**:619–24. doi:10.1136/jnnp.2007.124651

Honnedevasthana Arun A, Connelly A, Smith RE, *et al.* (2021) Characterisation of white matter asymmetries in the healthy human brain using diffusion MRI fixel-based analysis. *Neuroimage* **225**:117505. doi:10.1016/j.neuroimage.2020.117505

Hughes C, Berg L, Danziger W (1982) A new clinical scale for the staging of dementia. *Br J Psychiatry* **140**:566–72. doi:10.1192/bjp.140.6.566

Jacobs HIL, Van Boxtel MPJ, Jolles J, *et al.* (2012) Parietal cortex matters in Alzheimer's disease: an overview of structural, functional and metabolic findings. *Neurosci Biobehav Rev* **36**:297–309. doi:10.1016/j.neubiorev.2011.06.009

Joko T, Washizuka S, Sasayama D, *et al.* (2016) Patterns of hippocampal atrophy differ among Alzheimer's disease, amnestic mild cognitive impairment, and late-life depression. *Psychogeriatrics* **16**:355–61. doi:10.1111/psyg.12176

Jung J, Kang J, Won E, *et al.* (2014) Impact of lingual gyrus volume on antidepressant response and neurocognitive functions in Major Depressive Disorder: a voxel-based morphometry study. *J Affect Disord* **169**:179–87. doi:10.1016/j.jad.2014.08.018

Kozlovskiy SA, Pyasik MM, Korotkova AV, *et al.* (2014) Activation of left lingual gyrus related to working memory for schematic faces. *Int J Psychophysiol* **94**:241. doi:10.1016/j.ijpsycho.2014.08.928

Leyhe T, Reynolds CF, Melcher T, *et al.* (2017) A common challenge in older adults: classification, overlap, and therapy of depression and dementia. *Alzheimer's Dement* **13**:59–71. doi:10.1016/j.jalz.2016.08.007

Lin A-L, Laird AR, Fox PT, *et al.* (2012) Multimodal MRI neuroimaging biomarkers for cognitive normal adults, amnestic mild cognitive impairment, and Alzheimer's disease. *Neurol Res Int* **2012**:907409. doi:10.1155/2012/907409

Linnemann C, Lang UE (2020) Pathways connecting late-life depression and dementia. *Front Pharmacol* **11**:279. doi:10.3389/fphar.2020.00279

Liu Y, Spulber G, Lehtimäki KK, *et al.* (2011) Diffusion tensor imaging and tract-based spatial statistics in Alzheimer's disease and mild cognitive impairment. *Neurobiol Aging* **32**:1558–71. doi:10.1016/j.neurobiolaging.2009.10.006

López-Vicente M, Lamballais S, Louwen S, *et al.* (2021) White matter microstructure correlates of age, sex, handedness and motor ability in a population-based sample of 3031 school-age children. *Neuroimage* **227**:117643. doi:10.1016/j.neuroimage.2020.117643

Machulda MM, Lundt ES, Albertson SM, *et al.* (2019) Neuropsychological subtypes of incident mild cognitive impairment in the Mayo Clinic Study of Aging. *Alzheimer's Dement* **15**:878–87. doi:10.1016/j.jalz.2019.03.014

Association American Psychiatric (2013) Diagnostic and statistical manual of mental disorders: DSM-5. 5th. Washington, D.C: American Psychiatric Publishing.

McKhann GM, Knopman DS, Chertkow H, *et al.* (2011) The diagnosis of dementia due to Alzheimer's disease: recommendations from the National Institute on Aging-Alzheimer's Association workgroups on diagnostic guidelines for Alzheimer's disease. *Alzheimer's Dement* **7**:263–9. doi:10.1016/j.jalz.2011.03.005

Rabinovici GD, Gatsonis C, Apgar C, *et al.* (2019) Association of amyloid positron emission tomography with subsequent change in clinical management among Medicare beneficiaries with mild cognitive impairment or dementia. *JAMA* **321**:1286–94. doi:10.1001/jama.2019.2000

Ramos Bernardes da Silva Filho S, Oliveira Barbosa JH, Rondinoni C, *et al.* (2017) Neuro-degeneration profile of Alzheimer's patients: a brain morphometry study. *NeuroImage: Clinical* **15**:15–24. doi:10.1016/j.nicl.2017.04.001

Ran S, Zuo Z, Li C, *et al.* (2020) Atrophic corpus callosum associated with altered functional asymmetry in major depressive disorder. *Neuropsychiatr Dis Treat* **16**:1473–82. doi:10.2147/NDT.S245078

Ribeiz SRI, Duran F, Oliveira MC, *et al.* (2013) Structural brain changes as biomarkers and outcome predictors in patients with late-life depression: a cross-sectional and prospective study. *PLoS ONE* **8**:e80049. doi:10.1371/journal.pone.0080049

Salvador R, Canales-Rodríguez E, Guerrero-Pedraza A, *et al.* (2019) Multimodal integration of brain images for MRI-based diagnosis in schizophrenia. *Front Neurosci* **13**:1203. doi:10.3389/fnins.2019.01203

Sun X, Salat D, Upchurch K, *et al.* (2014) Destruction of white matter integrity in patients with mild cognitive impairment and Alzheimer disease. *J Investig Med* **62**:927–33. doi:10.1097/JIM.0000000000000102

Tabatabaei-Jafari H, Shaw ME, Cherbuin N (2015) Cerebral atrophy in mild cognitive impairment: a systematic review with meta-analysis. *Alzheimer's Dement* **1**:487–504. doi:10.1016/j.dadm.2015.11.002

Tzourio-Mazoyer N, Landeau B, Papathanassiou D, *et al.* (2002) Automated anatomical labeling of activations in SPM using a macroscopic anatomical parcellation of the MNI MRI single-subject brain. *Neuroimage* **15**:273–89. doi: 10.1006/nimg.2001.0978

Wen M-C, Steffens DC, Chen M-K, *et al.* (2014) Diffusion tensor imaging studies in late-life depression: systematic review and meta-analysis. *Int J Geriatr Psychiatry* **29**:1173–84. doi:10.1002/gps.4129

Whitfield-Gabrieli S, Nieto-Castanon A (2012) Conn: a functional connectivity toolbox for correlated and anticorrelated brain networks. *Brain Connectivity***2**:125–41. doi: 10.1089/brain.2012.0073

Whitwell JL, Dickson DW, Murray ME, *et al.* (2012) Neuroimaging correlates of pathologically defined subtypes of Alzheimer's disease: a case-control study. *Lancet Neurol* **11**:868–77. doi:10.1016/S1474-4422(12)70200-4

Wu JC, Buchsbaum MS, Johnson JC, *et al.* (1993) Magnetic resonance and positron emission tomography imaging of the corpus callosum: size, shape and metabolic rate in unipolar depression. *J Affect Disord* **28**: 15–25. doi: 10.1016/0165-0327(93)90073-s

Yendiki A, Panneck P, Srinivasan P, *et al.* (2011) Automated probabilistic reconstruction of white-matter pathways in health and disease using an atlas of the underlying anatomy. *Front Neuroinformatics* **5**:23. doi:10.3389/fninf.2011.00023

Yesavage JA, Sheikh JI (1986) Geriatric depression scale (GDS). *Clin Gerontol* **5**:165–73. doi:10.1300/J018v05n01_09

Yuen GS, Gunning-Dixon FM, Hoptman MJ, *et al.* (2014) The salience network in the apathy of late-life depression. *Int J Geriatr Psychiatry* **29**:1116–24. doi: 10.1002/gps.4171

Zhang A, Leow A, Ajilore O,, *et al.* (2012) Quantitative tract-specific measures of uncinate and cingulum in major depression using diffusion tensor imaging. *Neuropsychopharmacol* **37**:959–67. doi:10.1038/npp.2011.279

Zubenko GS, Zubenko WN, Mcpherson S, *et al.* (2003) A collaborative study of the emergence and clinical features of the major depressive syndrome of Alzheimer's disease. *Am J Psychiatry* **160**:857–66. doi:10.1176/appi.ajp.160.5.857

Received: 17 February 2023; **Revised:** 19 May 2023; **Accepted:** 12 June 2023